

EDITOR'S PAGE

IRON ORE SINTERING

PART 1. THEORY AND PRACTICE OF THE SINTERING PROCESS

SINTERIZACIÓN DE MINERALES DE HIERRO PARTE 1. TEORÍA Y PRÁCTICA DEL PROCESO

ALEJANDRO CORES

Ph. D., Centro Nacional de Investigaciones Metalúrgicas CSIC-CENIM, Spain, alcores@cenim.csic.es

LUIS FELIPE VERDEJA

Ph. D. Escuela Técnica Superior de Ingenieros de Minas, Oviedo, Spain, lfv@etsimo.uniovi.es

SERAFÍN FERREIRA

Ph. D., Centro Nacional de Investigaciones Metalúrgicas CSIC-CENIM, Spain, serafin@cenim.csic.es

ÍÑIGO RUIZ-BUSTINZA

Ph. D., Centro Nacional de Investigaciones Metalúrgicas CSIC-CENIM, Spain, irbustinza@cenim.csic.es

JAVIER MOCHÓN

Ph. D., Centro Nacional de Investigaciones Metalúrgicas CSIC-CENIM, Spain, jmochon@cenim.csic.es

Received for review June 5th, 2013, accepted July 3th, 2013, final version July, 12th, 2013

ABSTRACT: Sintering is a process by which a mixture of iron ores, fluxes and coke is agglomerated in a sinter plant to manufacture a sinter product of a suitable composition, quality and granulometry to be used as burden material in the blast furnace. This process is studied and researched in the steelmaking industry in general, and in sinter plants in particular, as well as in universities and metallurgical research centres throughout the world. As a result of this research, and the experience accumulated over many years, the sintering process is well understood. Nevertheless, despite this good knowledge of sintering, there are still a number of issues that need to be studied. The present work provides information on the iron ores that form part of the mineral mix which, once granulated, is loaded onto the sinter strand where it is partially melted at a temperature of between 1250-1350 °C and undergoes a series of reactions that give rise to the formation of sinter; a material of a suitable composition and strength to be loaded into the blast furnace to produce pig iron.

KEYWORDS: Sintering, Iron Ores, Coke, Granulation, Flame Front, Softening and Melting, Blast Furnace

RESUMEN: La sinterización es un proceso en el cual una mezcla de minerales de hierro, fundentes y coque se aglomera en una planta de sinterización para la fabricación de un producto de una composición, calidad y granulometría adecuada para ser utilizado como material de carga en el alto horno. Este proceso se estudia e investiga en la industria de fabricación de acero en general, en las plantas de sinterización en particular, así como en universidades y centros de investigación metalúrgicos de todo el mundo. Como resultado de esta investigación y la experiencia acumulada durante muchos años, el proceso de sinterización se conoce bien, sin embargo, a pesar de este buen conocimiento de la sinterización, todavía hay una serie de cuestiones que necesitan ser estudiadas. El presente trabajo proporciona información sobre los minerales de hierro que forman parte de la mezcla de minerales que, una vez granulada, se carga en la banda de sinterización en la que se funde parcialmente a una temperatura de entre 1250 - 1350 °C y en la que se producen una serie de reacciones que dan lugar a la formación del sinter, un material de una composición y resistencia adecuada para su utilización en el horno alto en la producción de arrabio.

PALABRAS CLAVE: Sinterización, Minerales de hierro, Coque, Granulación, Frente de llama, Reblandecimiento y fusión, Horno Alto

LIST OF ABBREVIATIONS

AIME American Institute of Mining, Metallurgical and Petroleum Engineers, (USA).

AIST Association for Iron and Steel Technology, (USA).

APD Anionic polymer dispersant.

ATS Association Technique de la Sidérurgie Française.

BF Blast furnace.

BIF Banded iron formation

BHP	Broken Hill Proprietary, (Australia)
CRM	Centre de Recherches Métallurgiques, (Belgium)
CSC	China Steel Corporation
DCM	Dry circuit material
DTA	Differential thermal analysis
EPMA	Electron probe microanalysis
FFS	Flame front speed
ICHEME	The Institution of Chemical Engineer, (UK)
ISIJ	Iron and Steel Institute of Japan
ISS	Iron and Steel Society, (USA)
JFE Steel	Formely named NKK
JPU	Japanese permeability unit
MEBIOS	Mosaic embedding iron ore sintering
NKK	Nippon Kokan Keihin
NSC	Nippon Steel Corporation
SAIL	Steel Authority of India Limited
SFCA	Silico-ferrite of calcium and aluminium
SFCAM	Mg-rich SFCA
SP	Sinter plant
VDEh	Verein Deutscher Eisenhüttenlente, (Germany)
XRD	X-ray diffraction
X-ray CT	X-ray computed tomography

1. INTRODUCTION

The sintering process is used to agglomerate a mix of iron ores (natural or synthetic), return fines, fluxes and coke, with a particle size of <8 mm, so that the resulting sinter, with a screened size of 12-35 mm, can withstand pressure and temperature conditions in the blast furnace [1-7].

The first stage of sintering is granulation of the raw mix, which consists of its homogenisation in a mixing drum for several minutes with the addition of 6-8% water. The granulated mix is then loaded onto the permeable sinter strand grate. The bed top is heated to high temperature by oil or gas burners and air is drawn through the grate. After a short ignition time, heating of the bed top is discontinued and a narrow combustion zone (flame front) moves downwards through the bed, heating each layer successively. In the bed the granules are heated to 1250-1350 °C to achieve their softening and then partial melting. In a series of reactions a semi-molten material is produced

which, in subsequent cooling, crystallises into several mineral phases of different chemical and morphological compositions; mainly hematite, magnetite, ferrites and gangue composed mostly of calcium silicates. The process energy, of the order of 1500-2000 MJ t⁻¹ of sinter [1], is supplied by combustion of the coke. Ahead of the combustion zone, water evaporates and volatile substances are driven off. In the combustion zone, reactions take place which give rise to the formation of a strong agglomerate. Most of the heat from the gases leaving the combustion zone is absorbed for drying, calcination and preheating of lower layers of the bed. When the combustion zone reaches the base of the bed, the process is complete and the sinter cake is tipped from the grate, roughly broken up and screened.

Sintering is a continuous process. The sinter strand is formed by a series of pallets, each of which has side walls and a permeable grate, which are loaded with the granulated sinter mix, pass under the ignition hood, are subjected to draught suction, tipped, and then return to the loading position. After being tipped off the pallets, the sinter is hot screened and the fine fraction (return fines, <5 mm) is recycled to be mixed with the raw materials while the coarse fraction is cooled and sent to the blast furnace hoppers. The wind boxes below the strand are connected to a fan via a gas scrubbing system.

The sinter production of nine Western European countries is around 100 million tonnes/year. (Austria: 2 SP; Belgium: 4 SP; Finland: 1 SP; France: 6 SP; Germany: 9 SP; Italy: 3 SP; Netherlands: 3 SP; Spain: 2 SP and United Kingdom: 4 SP).

2. RAW MIX

The raw mix that forms the sinter bed is comprised mainly of iron ores, coke, fluxes and return fines. The behaviour of the raw mix during sintering and the quality of the manufactured sinter depends largely on the chemical, granulometric and mineralogical composition of the iron ores. Understanding the impact of ore characteristics on sintering behaviour is important when it comes to selecting the most suitable raw mix for a given set of operating conditions.

Research into the influence of the raw mix composition on sinter phases has determined the influence of basicity

(CaO/SiO₂), temperature, thermal regime and Al₂O₃ and MgO contents on the ferrites content, total hematite, reoxidised hematite oxidised from magnetite, reducibility index (RI), reduction degradation index (RDI) and tumbler index (TI), porosity and coke rate [8-10].

2.1. Iron Ores

Western Europe and North America import high quality dense hematite ores from South America for their sinter plants. In Asia the ironmaking industry uses porous iron ores imported from Australia, which are poorer in quality than dense hematite ores.

Since the 1980's Japanese steel mills have paid great attention to the development of suitable sintering technology to allow the use of raw mixes with high goethite ore contents. Studies have been carried out on

melt properties during assimilation, the behaviour of raw mixes with high goethite ore contents, and on bed structure and permeability [11-12]. Japan and Australia are making great efforts to incorporate Australian ores in their sintering beds without affecting sinter plant performance indicators like productivity, coke rate, yield and sinter properties. In Australia the basic mineralogy of West Angelas iron ore, from a mine operated by Rove River Iron Associates, is a simple association of martite and goethite, in common with many Brockman type iron ores [13,14]. Marra Mamba ores present a wide range of lithological and mineral types from hard/dense to soft/highly porous and from martite to goethite and ochreous goethite. The softest ores can produce a high proportion of ultrafine particles (up to 30% <0.15 mm). Figure 1 shows the variety of ores found in the West Angelas deposit [13].

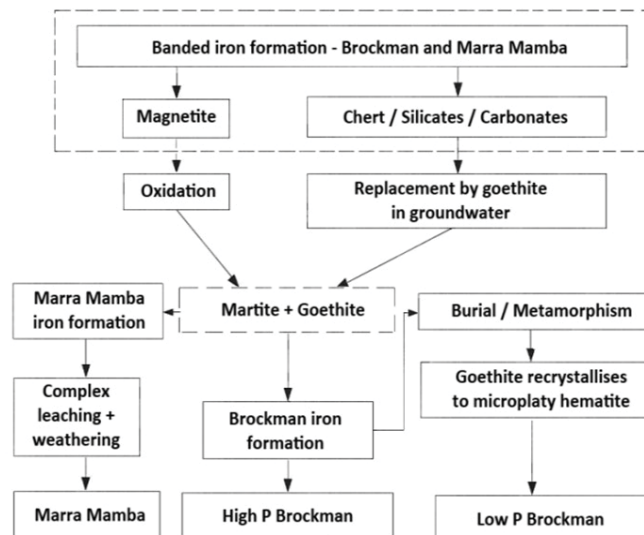


Figure 1. Simplified genetic relationship of Hamersley province (Australia) BIF derived iron ores

In 2001 ISIJ began a research project on meso-mosaic texture sinter with the aim of improving sintering when incorporating Australian goethite/limonite ores, broadly divided into Marra Mamba and pisolitic ores, in the raw mix [15,16]. Research was carried out by a working group of 10 members from 5 universities and 16 members from 6 Japanese integrated steelmakers. The project was split into 4 different research groups:

- G I. Characterisation and granulation of iron ores.
- G II. Characterisation of melt and mineral phase.
- G III. Quantification of the sintering process.
- G IV. Composite and bed designs.

As a result of this work a new agglomeration concept known as the MEBIOS process (mosaic embedding iron ore sintering) was proposed. In MEBIOS granulation the raw materials are distributed in the sinter bed following a meso-mosaic pattern. This technology is used to obtain assimilation control to form sinter beds with well developed voids and few pores (Fig. 2) [16]. In MEBIOS, the raw materials are granulated in two separate blends and the bed is formed by distributing the two separate raw materials beds in the form of a mosaic. The first blend, based on pisolitic limonite ore blended with coke and CaO, forms an induction bed that promotes smelting assimilation. The second,

based on Marra Mamba ore and consisting of fine and coarsely granulated material, is an ageing bed that suppresses smelting assimilation. It is considered that this distribution allows an ideal void network to form during normal sintering operation (Fig. 3) [16].

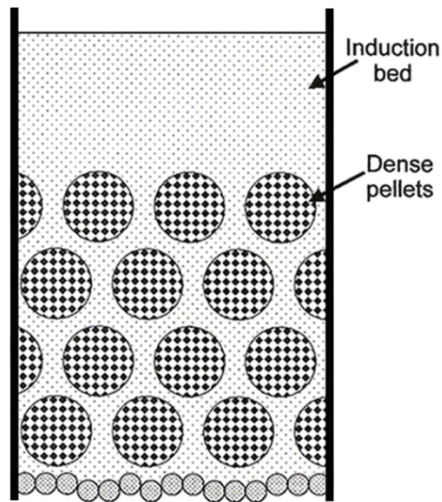


Figure 2. An image of the design of bed structure of raw materials

A research has been carried out to design pellets for the sintering, as the MEBIOS process, with less amount of liquid phase formation [17]. Pellets 15 mm in diameter are made with Marra Mamba fine particles ore and form the dense ageing bed. The porous induction bed is made with pisolitic ore. In the test carried out in a 90 mm diameter and 100 mm in height sinter pot, the ratios $\text{CaO}/\text{Fe}_2\text{O}_3$ and CaO/SiO_2 and temperatures are varied. Liquid phase ratio in the $\text{CaO}-\text{Fe}_2\text{O}_3-\text{SiO}_2$ system was about 40%, to achieve pellets with the best crushing strength, apparent density and the coalescing with the induction bed properties.

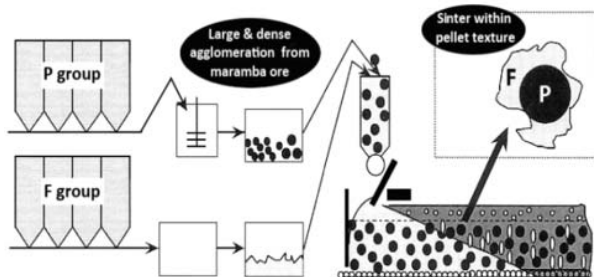


Figure 3. Image example of MEBIOS process

In tests [15] carried out in a 300 mm diameter sinter pot, using a bed with a 34% blend ratio of green pellets with Marra Mamba ore of 10-15 mm in diameter

granulated by the MEBIOS method, comparison of the manufactured sinters with others produced in ordinary conditions showed that MEBIOS improves ventilation properties by reducing the bulk density of the bed and increasing the overall bulk density of the raw material bed, although the product yield was lower due to insufficient bonding of the coarse granules. It was concluded that a thorough study on raw material granulation design and raw material bed design was needed in the future.

At BHP Billington's Newcastle Technology Centre in Australia, fundamental research has been carried out, with bench-scale experiments and sinter-pot test results, to understand the behaviour of goethite ores in sintering [18]. One Brockman hematite ore and two goethite ores (pisolitic and Marra Mamba) have been studied, with the latter forming up to 30% of the raw mix to be sintered.

The research has focused on sinter plant performance indicators, concluding that with adequate treatment goethite ores may be used without deteriorating the manufactured sinter.

Research has also been carried out on the mineralogy, granulability and melting characteristics of Marra Mamba ore [19]. It has been compared with hematite ore from Brazil, low-P Brockman hematite ore from Australia, pisolite ore and goethite ore from India. Marra Mamba ore is noted for its high porosity, the low cohesive strength of its quasiparticles, and the high moisture content necessary for its granulation. It has been used in sinter plants at rates of up to 100 kg t^{-1} of sinter, but the influence of Marra Mamba ores on current sintering operation is unclear.

The granulation behaviour of four raw mixes incorporating up to 30% Marra Mamba ore has been studied, using one Marra Mamba ore, two pisolite ores, four hematite ores and one concentrate in different proportions [20]. Besides the nature of the ores in the mix, the moisture content is another very important parameter, and the bed permeability and granulometric distribution of the mixes were determined for different moisture contents. It was seen that replacing a dense hematite ore with the porous Marra Mamba ore caused the bed permeability to improve when the moisture content was slightly higher.

The ultrafines content in an ore blend, particularly the <50 μm fines fraction, play a vital role in granulation, firstly in initiating the formation of a coating layer around the nucleus particles and then in binding together the larger-sized adhering fines with the coating.

Three Marra Mamba ores, one hematite ore and one pisolite ore, with different combined water contents and apparent densities, have been used to determine the quasiparticle nucleus properties required to manufacture sinters using limonite ores [21]. The porosity of the ores was determined after dehydration at 1200-1350 $^{\circ}\text{C}$. Assimilation of the nucleus of these ores was studied in samples prepared by surrounding the nucleus with a shell layer of a mix of CaO and Fe_2O_3 , in the 1200-1350 $^{\circ}\text{C}$ interval. As can be seen in Figure 4, limonite particles are more easily assimilated than hematite nucleating particles, but have an adverse effect on the melt fluidity.

The assimilation rate was seen to increase with the ore porosity, which in turn increases with the combined water content. If the solid phase ratio in the melt formed at 1250 $^{\circ}\text{C}$ is established at 10%, in order to maintain the fluidity of the system, the nucleus must be formed by dense particles with a maximum diameter of 15 mm.

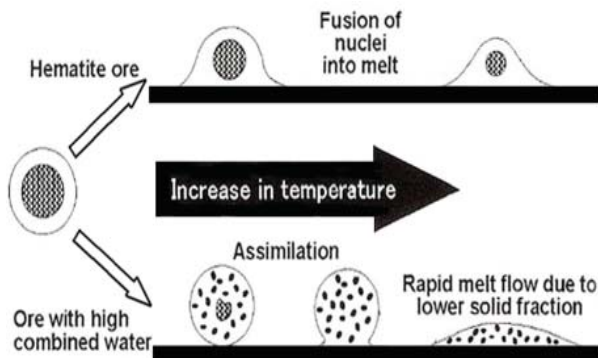


Figure 4. Assimilation of iron ore during sintering

The sintering behaviour of three Marra Mamba type iron ores has been studied [22] in a pilot plant by sintering in various operating conditions in combination with different proportions of four Brazilian ores, two Australian hematite ores and one pisolite ore. In certain conditions the use of Marra Mamba ores improved several parameters of the manufactured sinters.

The effect of the ore blend composition on sintering properties has been studied using mixes prepared with

different proportions of ten hematite ores and one pisolite ore [23], manufacturing sinters in a pilot plant with the same basicity and SiO_2 and MgO contents. When sinters were manufactured with the individual ores, sintering properties (productivity, moisture, coke rate, RI, RDI and TI) varied greatly with the iron ore type. When two ores were mixed, most of the sintering properties, except the RDI, were approximately equal to the weighted means of the individual ores. When mixes were made with increasing amounts of pisolite ore [23], sinter productivity decreased on average by approximately 1.3% for each 10% mass pisolite ore increase, depending on the ore type replaced by the pisolite ore, and a higher coke rate and more moisture in the raw mix were required. Attention is drawn to the notable influence of the Al_2O_3 content in the ores on sinter properties.

Figure 5 shows the evolution of iron ore production in Hamersley Province, Western Australia, showing a strong increase in production from 2000 to 2010 [24].

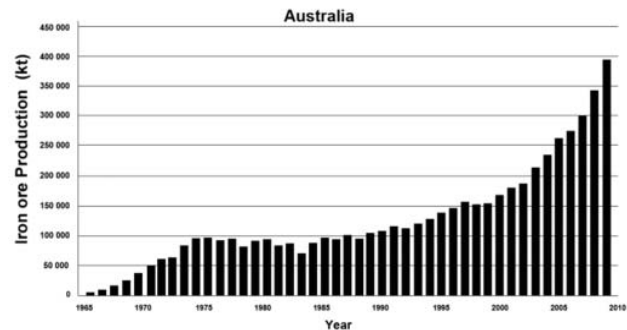


Figure 5. Australian iron ore production

2.2. Coke

Coke is the best fuel for iron ore sintering. Size classification is a crucial factor, and research has shown that the best economy and efficiency is obtained with a coke particle size of less than 3 mm [25], a product known as coke breeze. In Japan, studies have shown that the best coke size for sinter productivity and reducibility is between 0.25 and 3 mm [26]. Another study has determined that although a coke size of less than 0.25 mm has a negative effect on productivity, it does not affect the efficiency of the combustion process [27]. With regard to coke breeze, tests have shown the coarser fraction to be preferable and more economical in terms of consumption [26-28]. Comparison of different coke breeze size fractions has yielded better results with coarse coke (<3.15 mm and >1.00 mm) than with fine coke (<1.00 mm) [28]. Fine coke may be

considered mainly as adherent fines in granulation that form the surface coating around the grains. Fine coke burns quickly, while coarse coke burns more slowly and can widen the flame front, leading to a possible loss of productivity. Later tests have shown that a coarser fuel is more economical, reinforces sinter production, improves RDI and lowers SO₂ emissions.

The effect of the coke particle size in the sinter bed on productivity, coke consumption and sinter quality has been researched in sinter-pot tests [27]. It has been found that the coarser coke breeze fraction leads to a higher flame front speed and better combustion efficiency. Fine coke achieves poorer combustion efficiency, producing less heat and lowering the sintering temperature. As a result, the coke rate needs to be increased when finer coke is used in order to maintain sinter quality.

Research has also been carried out into the use of other fuels besides coke in sintering [29] determining the reactivity r (10⁵ g/g/s) of: coke 1 (2.20), coke 2 (1.09), black coal char (1.55), industrially produced charcoal (22.2), and black pine charcoal (419). The flame front speed (cm/min) has been found to increase as the reactivity rises:

$$\text{FFS} = 0.2014 \ln r + 4.039. \quad (1)$$

The most reactive coals are also seen to be less dense, and this favours an increase in the FFS. Productivity rises with reactivity, but the sinter obtained is less resistant because less melt is formed when fuel reactivity rises in sintering.

3. GRANULATION

The complete granulation process takes a time of approximately 30 min to 1 h, including the addition of moisture, granulation and insertion in the sintering machine. Granulation is of basic importance for the sintering of iron ores, as good sinter bed permeability largely determines the rate at which the process progresses and hence the productivity of the sinter plant. The first studies on the structure of granulated raw mixes were carried out at Nippon Steel Corporation (NSC) and coined the term “quasi-particle” [30,31].

A quasiparticle is composed of an iron ore nucleus, which during sintering remains partially unmelted,

surrounded by finer ore grains with silica gangue and in the presence of high basicity (CaO/SiO₂) (Fig. 6). Particles of >0.7 mm act as nuclei while particles of <0.2 mm act as adherent fines. The number of particles in the 0.2 to 0.7 mm range should be minimal as they affect the mix permeability in two different ways: (a) as nuclei they give rise to a smaller quasiparticle size, lowering the bed permeability; and (b) as adherent fines they are poorly bonded and easily separated from the dry particles [32,33]. Raising the water content added to the raw mix during granulation helps intermediate particles to adhere to the coarse nuclei, but they quickly become detached again during drying.

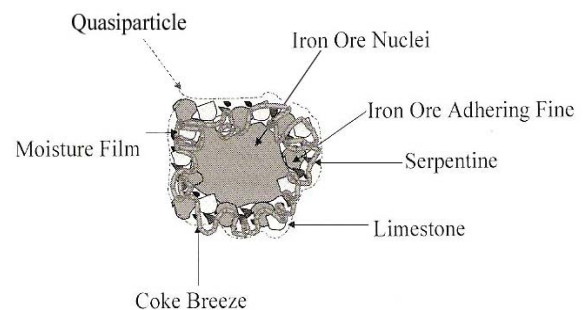


Figure 6. Quasi-particle schematic

A research has been carried out on the effect of micro-particles in 7 different iron ores on the optimum granulation moisture [34]. An anionic polymer dispersant (APD) accelerates micro-particles (<10µm and submicron size) dispersion in water with an increase in micro-particles content, resulting in strengthening the points of contact between the nuclear particles and fine particles or among the fine ones. The content of micro-particles in each granulometric fraction for ores is different. The extent of the increase in micro-particles by APD was varied with in iron ore type and the total amount of micro-particles was in the range from 2 to 10% in all ores. In Figure 7 it is considered that in the process of the change from the wet state to the dry state, micro-particles concentrate at the water bridge and ultimately form a solid bridge, thereby producing the force for keeping the fine particles stuck to the nuclear particles. When APD is added micro-particles in the iron ore are dispersed into water, causing the effective amount of liquid phase increase. As a result saturation degree increases, allowing for ore optimal granulation with a lesser amount of water.

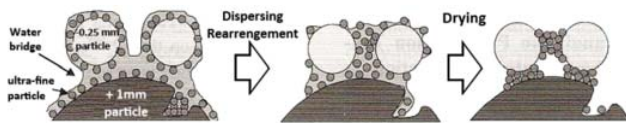


Figure 7. Behaviour of micro-particle on granulation

In sintering, ferrites form in the layer adhered to the nucleus due to the solid-liquid reaction between hematite and a $\text{CaO-Fe}_2\text{O}_3$ melt containing small amounts of SiO_2 and Al_2O_3 . Adhesion is highly influenced by the moisture available for granulation [32,33]. Other factors such as the nature of the nucleus, particle shape and surface properties are of secondary importance.

3.1. Moisture content

The moisture content in the raw mix to be sintered is a very important parameter in the granulation stage of sintering. The process of adhering fine particles to nuclei to form quasiparticles is very strongly influenced by the moisture available for granulation (total moisture minus moisture absorbed by sinter feed components) [32,33].

Maximum production is achieved with the optimum moisture addition, which is less than that required for maximum air permeability [35]. It is customary to operate at about 0.85 times the requirement for maximum permeability. This is because moisture condenses in the bottom layer of the bed after evaporating from the upper part as the flame front approached. Condensation is reported to take place during the first 2 min of sintering before the raw mix reaches its dewpoint temperature [36].

Good control of moisture addition is essential. Many plants have installed online infrared analysers to monitor the moisture content in the granulated feed. Water addition in the mixing drum is automatically adjusted to maintain the set moisture level [37]. Automatic control is preferred to manual methods since it assures a more rapid response and more consistent feed to the sinter strand [38].

3.2. Granulation fitness

The aim of granulation is to make the fine particles adhere to each other and form coarser particles. As a

result the granulated ore contains a smaller range of particle sizes, and consequently offers less resistance to the passage of the gases, thus improving bed permeability and plant productivity. Granulation is carried out in rotating drums. Rolling the materials in a drum increases the granule size by adhesion due essentially to the action of two types of forces: (a) “interlocking” of the particles; and (b) attraction by the creation of liquid phase “bridges” between the particles.

The importance of the magnitude of interlocking forces can be varied by altering the sequence of formation of the mix to be sintered so as to favour the aggregating action of the granulation nucleus provided by a given component (e.g. the return fines). The magnitude of interlocking forces can also be varied by modifying the sinter mix formation sequence to include a selective granulation or preagglomeration process [39-42]. In most cases this involves treating the ore fines and concentrates, some return fines and lime separately using an additional process line. These materials are mixed with water and micropelletised in a drum or disc before being introduced in the main granulation circuit prior to the granulating drum. This system has been installed by Nippon Kokan Keihin (NKK) in its No. 4 SP at Fukuyama [39]. In this process the return fines act as the nucleus and lime acts as the agglomerating agent. This practice allows the use of a greater amount of fines with no loss of productivity. In its No. 2 SP at Kashima, Sumitomo Metal Industries has developed selective granulation as a means of improving (lowering) the RDI [40]. In its sinter plant at Oita, NSC uses selective granulation to increase the goethite ore content in the raw mix [41,42].

Forces of the latter kind (bridges) are originated by the presence of water added to the mix, and their effect can be heightened by the use of additives. In both cases (interlocking and bridges) the strength of the granulated particles is not great, it is only sufficient to ensure that the granulated mix can be transported and layered on the sinter grate without breaking. The size distribution of a granulated mix when it is fed onto the sinter grate ranges from about 1 to 10 mm.

3.3. Structure of granules

The 3D X-ray tomography technique has been used to research the structure of the granules in three-

dimensional images [43]. Mixtures of iron ore fines (concentrates), return fines and limestone were prepared at concentrate/ore ratios of 20:80, 50:50, 80:20 and 100:0 and sinters manufactured with basicities of 0.8, 1.4 and 2.0. Incorporating increased amounts of concentrate in the sinter mix makes granulation more complex. Superfine particles not only adhere to coarse particles but may also form durable nuclei while binding particles of intermediate size, and the more superfines are used in the sinter mix, the less predictable the size distribution of the granules. Granules belonging to the sinter mix without coarse ore (concentrate/ore ratio of 100:0) had no nucleus and very few limestone particles stuck to the surface that is initially formed by the pelletising mechanism, and presented a similar structure to that of pellets. Granulating behaviour cannot be fully explained by any one single factor, such as the concentrate/ore ratio [44], and changes in the ore mineralogy, composition and amount of gangue, heat consumption and water content in the mix are also very relevant factors.

The 3D X-ray tomography technique has also been used to assess the porosity of these same sinters [45], and allows differentiation between open and closed pores. The porosity values obtained with this technique are higher than those obtained with the mercury intrusion method, due to the fact that the 3D technique offers the spherical diameter of the pores, while mercury characterises the pores by the diameter of mercury intrusion in the pore.

A system has been developed to determine the size of pseudo-particles in just a few minutes, without breaking the particle structure, by optical line scan technology [46]. The system consists of 4 modules: material feed; image acquisition; view processing; and control unit. It allows the granulation index of the process to be obtained.

To investigate the structure of a sinter bed in three dimensions the CT X-ray technique and 3D imaging analysing system is used [47]. The CT parameter is defined as a function of the X-ray absorption coefficients at the measured pixel and of the standard material (air). In a sinter pot of 90 mm in diameter and 400 mm in height, 4040×40 mm cubic samples of sinter are taken at three levels of the bed. In each sample a cluster of both pores and matrix of a volume close to

that of the sample is observed, with open pores. In the smaller clusters the pores are extremely small and closed. It is determined that, altogether, the sinter bed consists of a solid bed containing a multitude of closed pores of a diameter of less than 2 mm.

3.4. Granulation practice

Sinter productivity is directly related with bed permeability. In turn, permeability is related with the granule size distribution and average granule size, which are dependent upon the moisture addition. Permeability rises to a maximum value as a function of the moisture. Maximum productivity is obtained using 85% of the moisture required for maximum permeability due to the condensation of moisture in the bottom layer of the bed.

Research has been carried out to predict the granulation behaviour of a series of iron ores of different natures [44], proposing an equation to calculate the optimum moisture of the raw mix as a function of the nature, composition and granulometry of the ores. The optimum moisture content was defined as the lowest amount necessary to achieve maximum bed permeability. The equation was applied for each ore and ore mix, with the addition of coke, flux and return fines. Good correlation was found between experimental and calculated values.

In other research on granulation, equipment was designed to determine the moisture capacity of several iron ores and ore mixes [48]. The moisture capacity was defined as the maximum water content that can be retained between ore particles. It was seen that the moisture capacity increases in line with the external surface area and decreases as the ore pore volume rises. The ratio between the optimum moisture (W) and moisture capacity (mc) of a raw mix was determined as:

$$W = 6.94 + 0.12 mc \quad (2)$$

The experimental data indicated a very high correlation between W and mc. Continuing with this research [49], the following equation has been proposed, based on earlier work [44], to calculate the optimum moisture (W) as a function of the nature, composition and granulometry of the ore:

$$W = 2.28 + 0.427 L + 0.810 A - 0.339S + 0.104d_{-0.2 \text{ mm}} + 0.036I \quad (3)$$

Where:

L = ore weight loss during heating (g)

A = % alumina in ore

S = % silica in ore

$d_{-0.2 \text{ mm}}$ = ore size fraction less than 0.2 mm

I = ore size fraction between 0.2 and 1 mm.

It was established that a sample with a higher moisture capacity needs more water to achieve the best bed permeability. It has not been possible to directly relate permeability with the nature of the ore.

Research has been carried out into the effect of moisture addition and wettability on granulation by determining the contact angle between iron oxide and water and the iron ore granulation fitness [50]. The study considered one reagent grade hematite, three hematite ores and three goethite ores, determining interaction between the following parameters: nature of ore; porosity (range from 5 to 20); moisture content (11.8, 12.8 and 13.8% vol.); wettability time (0 to 20 min); measurement of ore-water contact angle by sessile drop method (50 to 100°); surface roughness (1.4 to 6.7 μm); rpm of pelletising machine (20, 30 and 40); adherent fine ratio (AR) of fine particles to nucleus (0 to 1); and fracture strength (FS) of quasiparticles (0 to 6). The best granulation is achieved with a goethite ore nucleus, with high porosity, low roughness and a low contact angle (more wetted).

The granulation behaviour of Thabazimbi and Sishen iron ores has been researched in proportions of 20:80 and 50:50 [51]. Four mixes of these ores were prepared with the addition of coke, limestone and return fines in order to determine the grain size distribution and average granule diameter before and after granulation. The permeability of each mix was experimentally determined in a unit with a height of 0.595 m and an internal diameter of 0.142 m, and the measured values were inserted in the following equation:

$$JPU = V / [A(H / \Delta P)^{0.6}] \quad (4)$$

Where:

JPU = Japanese Permeability Unit

V = air flow (Nm^3/min)

A = area (m^2)

H = bed height (mm)

ΔP = applied suction through bed ($\text{mm H}_2\text{O}$)

The bed permeability was determined for each mix as a function of the water content and granulation time. Sinters were manufactured and a relationship was established between the granule characteristics, bed permeability and sinter quality indices.

3.5. Two-stage granulation

Alongside the existing granulation equipment in its No. 4 and No. 5 SPs at Wakamaya (Japan), consisting of two drum mixers in serie, Sumitomo Metal Industries has added a preliminary granulation stage consisting of a mixer with a high stirring rate followed by a drum mixer [52]. This two-stage granulation system has made it possible to treat fine ores while increasing the flame front speed, permeability and productivity of the process (Fig. 8).

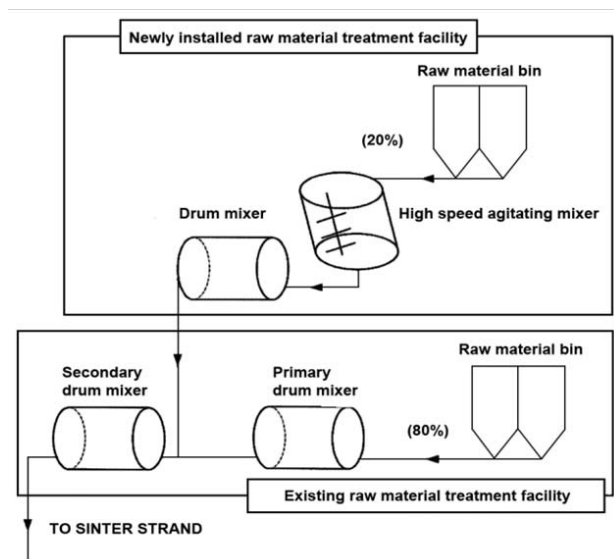


Figure 8. Outline of newly installed facility at Wakamaya No. 4 SP

Tata Steel (India) has implemented a two-stage granulation process to introduce dry circuit material (DCM) fines with a 1.83% Al_2O_3 content in proportions of 10 to 25% in the normal mix formed by Naomundi and Joda iron ores with 2.46% Al_2O_3 . In the first stage the DCM fines are granulated with water and lime in the form of micropellets, and in the second stage they are added to the normal mix and granulated [53].

Sintering with 20% DCM fines lowers the alumina content from 2.62% (base mix without DCM fines) to 2.47%, improving productivity and the RI and RDI indices. For the smooth operation of its blast furnace, Tata Steel established that RDI was the most critical sinter property, and accordingly identified the need to lower the alumina content in sinter.

3.6. Coating granulation

It is advantageous to improve the conventional granulation process, especially when using goethite and limonite ores which usually present a higher Al_2O_3 content than hematite and lead to deterioration of sinter properties. In this respect, research has shown that sinter improves when the conventional granulation stage in the drum mixer is followed by a second stage [54]. In the first stage the mix of iron ore and return fines is placed in the drum. In the second stage, coke plus limestone plus dolomite is added to the mix resulting from the first stage and the granule obtained is formed by a nucleus composed mostly of iron ore surrounded by coke and flux.

This coating granulation process [54] improves the flux formation reaction due to the segregation of CaO from the limestone on Fe from the iron ore. This makes sintering take place at a lower temperature, improves permeability and productivity, and decreases the formation of secondary hematite, with the consequent improvement in the RDI. The TI and reducibility also improve, due to the formation of more micropores, which also prevent the propagation of cracks responsible for deterioration of the RDI. The mixing time in the drum in the second stage is very important, and around 50 seconds has been established as the optimum time. A shorter time does not allow the nucleus to become well coated with coke + flux. A longer time causes destruction of the quasi-particles, due to the inclusion of coke and flux in the granules (of the nucleus), and yields a similar quasi-particle to that obtained in single-stage conventional granulation.

JFE Steel (Japan) has carried out a highly detailed study on the coke and limestone coating granulation method at Kurashiki No. 2 SP and No. 2 BF with the aim of improving productivity, reducibility and blast furnace operation [55]. This technology consists of coating coke and limestone on the surface of quasi-particles that

have been granulated in the primary part of the drum mixer. Coke and limestone are injected from the end of the drum mixer by the belt conveyor at high speed to achieve their coating on the quasi-particles. The coating granulation time is the most important control factor and is adjusted by changing the conveyor speed. The best time is in the 40-60 s range; with shorter times not all the quasi-particle is coated, and with longer times the quasi-particle is destroyed (Fig. 9).

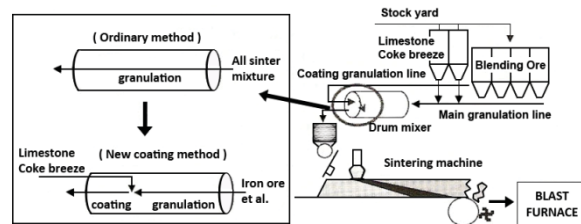


Figure 9. Process flow of coke and limestone coating granulation technology at Kurashiki No. 2 SP

Tests have been carried out [55] to assess the segregation of particles granulated separately (coke coating and limestone coating), and in both granulations productivity has been seen to rise compared to conventional productivity. Coke coating improves the cohesion stress of quasi-particles and thus improves permeability in the wet zone. With limestone coating the sinter presents a lower secondary hematite content and a structure with crack tolerance (improved RDI), more primary hematite and SFCA (improved RI), and improved melt fluidity. In the blast furnace, shaft efficiency improves by 1%, and the reducing agent rate can be lowered by 7 kg t⁻¹ of HM.

3.7. Selective granulation

NSC installed selective granulation technology in its No. 2 SP at Oita in 1995 and in its No. 3 SP at Yawata in 1996 [42,56]. This process is used to allow the sintering of iron ores with high alumina content, which are otherwise difficult to sinter due to the low reactivity of alumina-bearing materials and the high viscosity of primary melts. Selective granulation consists of screening the ore and sending the larger size fraction which has a lower alumina content to the conventional granulation circuit, while the smaller size fraction with a higher alumina content is pelletised into 2-5 mm granules which are incorporated in the conventional granulation circuit. The smaller size fraction contains

clayish ores that are high in alumina and require higher melting temperatures.

Laboratory research has been carried out [42] using ores with a 0.2% to 3.2% Al_2O_3 content to study the formation of the primary melt resulting from reaction of the ore fines with limestone. It has been shown that selective granulation achieves a granule nucleus with a higher alumina content than conventional granulation. With this process, the fines adhered to the nucleus, with a lower alumina content, by reacting with the limestone, promote the formation of the primary melt at a lower temperature.

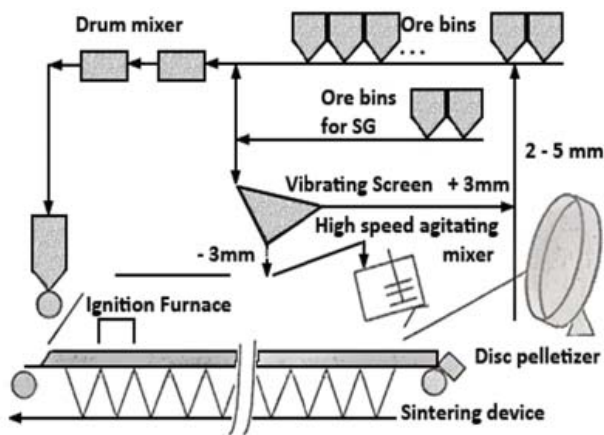


Figure 10. Process flow of selective granulation equipment

Figure 10 shows the selective granulation equipment installed in the No. 2 SP at Oita [42]. This process has a high raw materials processing rate of 300 t h^{-1} , and can process sticky raw materials continuously for 24 hours without operators. A fuel coke reduction of 3.8 kg t^{-1} of sinter and a blower power reduction of 3.8 kW t^{-1} were achieved. Productivity was improved by 0.5 t m^{-2} per 24h and the FeO content was reduced by 1%. The improvement of reducibility in turn led to a reduction in coke consumption in the blast furnace.

Research has been carried out in the pilot plant on the influence of selective granulation on a series of iron ores with an Al_2O_3 content of 2 to 5.5% [57]. The ore is separated into two fractions: $>1 \text{ mm}$ (lower alumina content) for conventional granulation and $<1 \text{ mm}$ (higher alumina) for selective granulation. As the alumina content rises, the FeO content, TI and productivity all decrease. Alumina presents a highly adverse effect on the RDI, which rises as the alumina

content increases. With selective granulation the quality of each manufactured sinter improves.

4. FLAME FRONT

Flame front temperature has a very large impact on sintering time and productivity because its influence on flame front permeability. Results [58] show that reducing flame front temperature is very beneficial to productivity because the resistance of the flame front to airflow is a function of gas velocity to the power of three. Raising flame front temperature greatly increases airflow resistance and leads to increased sintering time and reduced productivity.

Measuring the temperature at different levels in the sinter bed allows the movement of the combustion zone to be monitored and the concept of the flame front speed to be defined as the rate at which the level where the fastest temperature rise takes place moves through the bed. Figure 11 shows the ideal heat distribution in the sinter bed. The heating time in the high temperature zone (above $1100 \text{ }^\circ\text{C}$) must be short (1.5 min) because the partial oxygen pressure measure p_{O_2} in this zone is low due to coke combustion and FeO, which

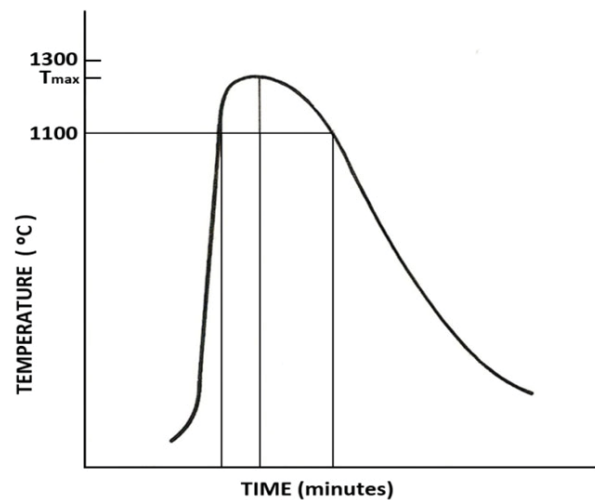


Figure 11. Ideal temperature profile of temperatures distribution in the sinter bed

is harmful to sinter reducibility, is easily formed. The cooling time (to $1100 \text{ }^\circ\text{C}$) must be long (from 3 to 5 min) in order to achieve a strong sinter structure by the formation of a gangue matrix, which is favoured with the presence of SiO_2 . Time-temperature profiles (Fig. 11) have been measured in several positions in the bed, and indicate that the width and T_{max} of the combustion zone increase as it drops through the

bed. In order to achieve a uniform T_{max} , double layer sintering is carried out in some plants, and consists of preparing the bed with a higher coke content in the upper layer than in the lower layer in order to counter the tendency of T_{max} to rise [59,60]. In addition to a double layer to control heat distribution in the bed, continuous measuring equipment has been developed which directly signals the temperature distribution throughout the bed, along with a device to measure the distribution of the volume sucked through the sinter grate [61]. The heat distribution can be controlled by adapting the strand speed and the coke content in the raw mix.

Tests have been carried out in a rapid heating furnace which allow the construction of a thermal profile of the sample (hematite + limestone) which simulates the profile of the sinter plant [62,63]. Sintering has been studied with the aid of simulation models and good correlation has been found between the experimental heat distribution and that calculated by the model [63,64]. In another study, an equation for heat distribution in the bed has been formulated, with good correlation between experimental and calculated data [65]. In a pilot plant it has been possible to achieve uniform heat distribution through the bed cross-section by means of automatic control of the load level, using an ultrasonic level meter that relates the gas temperature below the wind boxes with the load level [66]. Improvements have been achieved in efficiency, productivity and sinter quality.

In two sinter strands a model has been developed which combines the heat balance with the analysis of CO , CO_2 and O_2 in a wind box, allowing the development of a control system for the strand [67]. In this way it is possible to determine the position of the flame front, the T_{max} and the amount of liquid (melt) formed in the combustion zone. In laboratory research a model for combustion and heat transfer in the sinter bed has been proposed [68]. The data calculated by the model, from the profiles of curves corresponding to flame front propagation, combustion gas composition (CO , CO_2 and O_2) and coke content in the raw mix, are compared with experimental data from the sinter pot and good correlation is observed. In another study a model has been proposed to determine the flame front propagation rate through the bed. The main parameters of this research were coke combustion and the CO and CO_2 content and flow in the gas passing through the bed. Good correlation was found between the data obtained by the model and experimental results in a pilot plant [69].

4.1. Relation between maximum flame front temperature and sinter structure

When sintering is carried out at a temperature below $1300\text{ }^\circ\text{C}$, at around $1200\text{ }^\circ\text{C}$ a melt (consisting mainly of Fe_2O_3 and CaO) is generated in the sintering bed, and the iron oxide and fine particles are assimilated in the melt. If the melt penetrates the hematite grain, interfacial breakdown occurs, leaving a primary hematite (unmelted) that is considered beneficial for sintering because it improves the RI. When CaO and Al_2O_3 are assimilated in the melt, this reacts with the iron oxide and generates acicular calcium ferrite (of a size of less than $10\text{ }\mu\text{m}$) containing Al_2O_3 and SiO_2 as solid dissolutions, according to the general reaction:

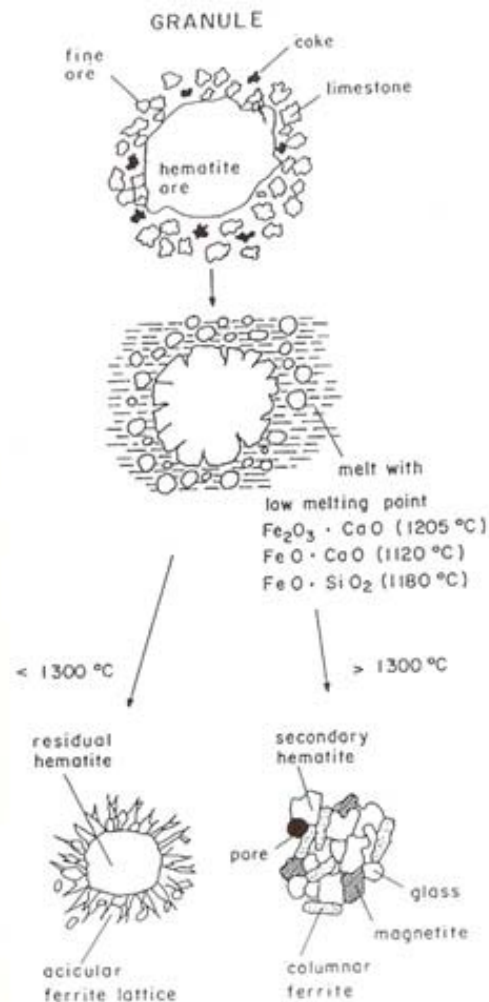
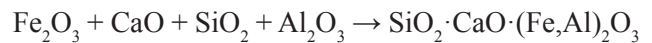


Figure 12. Development of sinter structure

These silicoferrites of calcium and aluminium (SFCA) are considered very beneficial components for the sinter structure since they possess good reducibility and afford the sinter mechanical strength, improving the shatter index (SI) and tumbler index (TI).

When sintering at low temperature (<1300 °C) the formation of magnetite decreases (less FeO) and sintering improves the RI and improves (lowers) the RDI. Furthermore, the optimum structure for sinter reducibility in the blast furnace is achieved, namely that formed by a hematite nucleus (unmelted) surrounded by an acicular ferrite network [59,62,70].

When sintering at a temperature above 1300 °C, part of the ferrite dissolves and melts to become converted into hematite or magnetite and into gangue components [71-73]. When the melt cools it forms as new phases large ferrite crystals, which reduce worse than acicular ferrite, and secondary hematite, which is detrimental to the RDI [70]. Figure 12 illustrates schematically the development of the different structures of sinter as a function of the T_{max} reached in the bed. In Table I it can be seen how the phase composition and sinter quality indices vary as a function of the T_{max} [74,75]. The best results are obtained in the 1225-1275 °C interval, with a maximum percentage of ferrites, high primary hematite, low secondary hematite, good porosity, and good quality indices (FeO, RDI, RI and SI).

5. SOFTENING AND MELTING

The blast furnace operation is dependent upon the geometry and situation of the cohesive zone, which is limited by the softening (ST) and melting (FT) isotherms [76-79]. The cohesive zone is constituted by alternate layers of soft sinter and coke. The latter, known as “coke windows”, allow the reducing gas to pass through to the upper areas of the furnace. It is therefore important for the cohesive zone to be as narrow as possible, in order to facilitate the penetration of the reducing gas, and as low as possible in the blast furnace, so that the furnace preparation zone above the cohesive zone is sufficiently large to allow the reduction of iron oxides. In order to fulfil both conditions the ST and FT must be as high as possible and the difference between them must be minimal.

Table 1. Approximate values of phase composition and sinter quality versus maximum temperature in the bed, %

	T_{max} , °C		
	1175-1225	1225-1275	1275-1350
Primary hematite	50	42	22
Secondary hematite	5	5	20
Magnetite	10	15	20
SFCA	35	38	30
Glass + 2CaO.SiO ₂	7	10	12
Porosity	35	30	15
FeO	3	4	5.5
RDI	30	32	36
RI	72	70	64
SI	93	94	95

Blast furnace coke consumption has fallen, partly to be replaced by pulverised coal injection through the tuyeres. Part of the coke saving, however, can be attributed to improved sinter quality, in particular its reducibility and high temperature properties.

Research has been carried out into the fundamental mechanism underlying the softening and melting of blast furnace sinter [80,91]. Figure 13 shows the sequence that takes place during softening and melting experiments: pre-softening, softening, exudation and dripping stage. The softening mechanism is related with the melting rate of the core as a function of temperature. Deformation is thought to be directly related with the macroporosity generated by the transfer of melt from the core to the shell. Initial melt formation plays a role in the start of softening, reduction, retardation and dripping of melt from the bed.

In India, Tata Steel uses coke with a high ash content (25-30%) in its blast furnaces. For the good operation of the furnaces it uses a sinter with a high basicity (2.50) and a high alumina and magnesia content: Fe_{total} 46.9%, FeO 8.9%, CaO 17.5%, SiO₂ 7.05%, Al₂O₃ 4.5% and MgO 5.2% [80]. In addition to sinter, the furnaces are loaded with Joda and Naomundi hematite ores (Fe_{total} 65%). In an experimental unit that reaches a maximum temperature of 1400 °C, the softening and melting of sinters is determined for different basicities (range 1.50 to 3.0), magnesia contents (range 3.3 to 10%) and sinter reducibility grades. The softening-melting range is defined as the temperature range between the point of reversal (T_1 softening) and 10% contraction (T_2 melting) in Figure 14. Furnace behaviour improves (lower and narrower cohesive zone) as the sinter/ore ratio in the load increases.

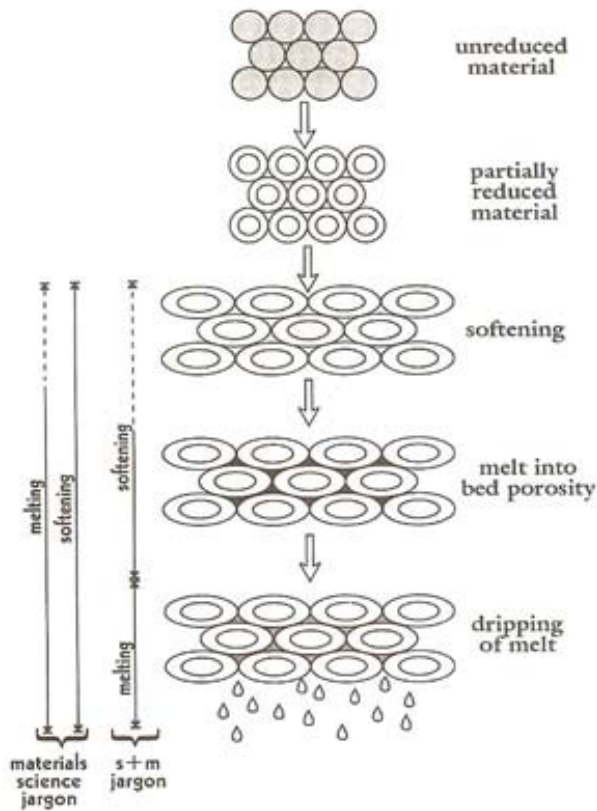


Figure 13. General sequence of events during typical bulk scale softening and melting experiment

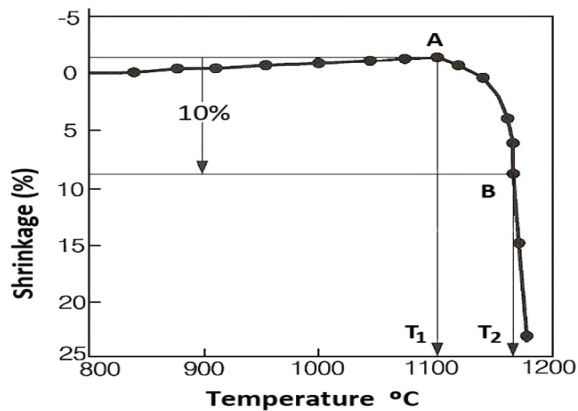


Figure 14. Actual shrinkage in the bed height during softening test of a typical sinter

Tata Steel also carried out research into the effect of the FeO content in sinter (sinter A 10% and sinter B 12.1%) on softening and melting, and its impact on the

blast furnace [83]. The sinter with more FeO caused early softening of the burden, a phenomenon that is undesirable in the blast furnace [84]. Unreduced FeO will be reduced at a higher temperature, according to $FeO + C \rightarrow Fe + CO$, and such direct reduction in a greater amount would lead to a higher coke rate in the process. A lower wind volume, production and productivity were also seen in comparison with furnace behaviour when operating with a sinter load with 10% FeO. A drop in the MgO content in sinter from 1.77 to 1.48% gives rise to changes in furnace behaviour which are attributed to variations in the softening and melting temperatures [83].

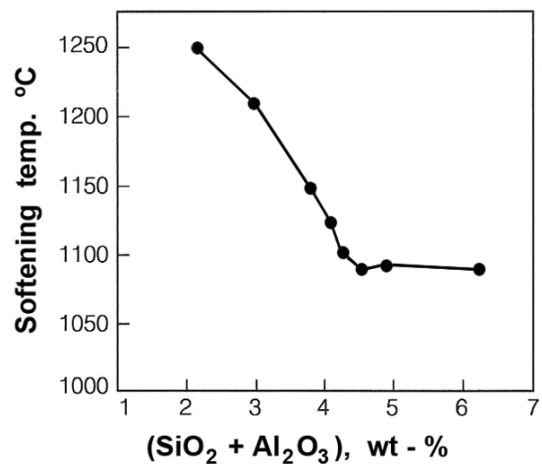


Figure 15. Influence of total gangue content on softening temperature

China Steel Corporation (CSC) has researched the influence of the material composition on softening and melting properties in No. 2 BF burden materials. The experimental part has been carried out in a unit that simulates blast furnace conditions, operating under load up to a temperature of 1580 °C, and both pilot plant and industrially manufactured sinters have been tested [85]. Sinter showed a high softening temperature (around 1400 °C) but a relatively low meltdown ratio and poor high temperature permeability. An increase in sinter basicity was seen to be detrimental to the fluidity of melted slag and iron in the furnace, resulting in more melted slag and iron being blocked in the coke layer, consequently decreasing the % meltdown and increasing the gas resistance of the sample bed. For this reason it is important to lower the sinter basicity. On the other hand, an increase in Al_2O_3 (range from 0.9 to 2.6%) or MgO lowered the slag melting point, thus favouring

a reduction in high temperature gas resistance. Sinter presents better softening and melting behaviour than pellets or ore, but worse meltdown and high temperature gas resistance. It has been seen that a mixed burden containing 65% sinter, 20% lump ore and 15% pellets is slightly better than other compositions in terms of FT-ST, meltdown and high temperature gas resistance.

Steel Authority of India Limited (SAIL), with its five integrated steel plants, has studied the softening temperature of a series of iron ores and sinters [86]. Figure 15 illustrates how the softening temperature comes down as the gangue content in the ore increases, due to the fact that gangue is formed by compounds with a low melting point: $2\text{FeO}\cdot\text{SiO}_2$, $\text{FeO}\cdot\text{SiO}_2\cdot\text{CaO}$, $\text{Fe}_2\text{O}_3\cdot\text{SiO}_2\cdot\text{CaO}$. The alkalis contained in gangue can also form compounds with a low melting point: Na_2SiO_3 , K_2SiO_3 , $\text{NaAlSi}_2\text{O}_6$. The softening temperature of the sinters manufactured in the different plants is between 1310 and 1350 °C, and depends on the composition and mineralogy of the sinter.

The permeability resistance K of the sinter bed is evaluated by the sinter softening property test. When K is plotted against the bed temperature, integrating the curve obtained in the 1000-1600°C interval, the KS bed resistance parameter may be calculated. It has been found [87] that a reduction in the SiO_2 content and an increase in MgO in sinter improves both its permeability (lower KS) and the sinter softening property. The action of SiO_2 is due to a decrease in the melt that fills the voids in the bed. The action of MgO is due to an increase in the melting point of $\text{CaO}\cdot\text{FeO}\cdot\text{SiO}_2$ slag. The Al_2O_3 content has little effect on the sinter softening property.

NSC has researched at Kimitsu No.3SP as the sinter is improved when a decreasing Al_2O_3 content from 1.85 to 1.50% was performed, by changing Australian high Al_2O_3 content ores in the raw mix to Brazilian low Al_2O_3 content ores [88]. Test operations at Kimitsu No. 3 and No. 4 BFs were performed. It was verified quantitatively that reducing Al_2O_3 content in sinter can better the reduction and softening-melting of sinter in the blast furnace. Also the permeability resistance index in the cohesive zone is improved. This may be because the amount of melt having low melting point being little owing to the improved reduction efficiency and lower Al_2O_3 content.

The softening and melting behaviour of three lump hematitic ores and a sinter has been determinate in a rig that operate under load [89]. Beds of lump ores contract much earlier than sinter by the formation of fayalite, with a low melting temperature considerate to be around 1177 to 1205 °C. No fayalite forms in sinter and at higher temperature melts that are generated appear to be more viscous, resulting in less bed deformation. There is not an appreciable difference for the softening and melting temperatures for sinter and for 80% sinter and 20% lump ore blend. With this blend as ferrous burden in the blast furnace, the permeability remained in the normal operating range, the same that when the BF operate with 100% sinter, with no indication of non-uniform gas flow conditions or abnormal cohesive zone issues and gas utilization efficiency even improved slightly.

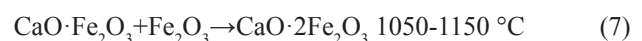
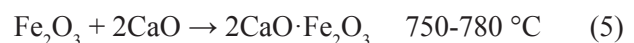
An important property of melts is that they coalesce, transforming the uniformly packed bed of granules into sinter particles and very large channels in the bed [18]. The coalescing behaviour of melts should have a favourable influence on flame front properties in determining the permeability of the sinter bed.

6. REACTIONS IN THE SINTERING PROCESS

In the sintering process the temperature of the raw mix is raised to achieve its partial melting and to produce a molten material which, during cooling, crystallises or solidifies into several mineral phases that agglomerate the structure as a whole. The energy for this process is supplied by combustion of the coke [9,89].

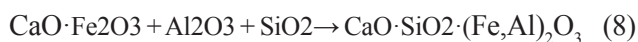
A study to determine the sequence of reactions in SFCA formation has been carried out using a combination of XRD, DTA and EPMA techniques [88].

The first ferrites formation reactions are solid-solid reactions that start at 750-780°C and end at 1200°C, the melting temperature of these ferrites, following the sequence dicalcium ferrite (C_2F) → calcium ferrite (CF) → calcium diferrite (CF_2):



Calcium oxide plays an extremely important role during sintering as it combines easily with iron oxides in the mix to produce calcium ferrites. The melt formation reaction starts at the point of contact between the ore fines and calcium oxide. At the same time, the solid-solid SFCA formation reaction starts at around 1050 °C and continues in a solid-liquid reaction above 1200 °C. The presence of Al₂O₃ increases the stability of SFCA, and lowers the temperature at which these ferrites start to form.

Above 1200 °C, solid-liquid (solid-melt) reactions predominate, with the presence of a molten phase that reinforces the assimilation of material to form ferrite:



The sequence of reactions [90] is shown in the diagram in Figure 16. Alumina is highly reactive and enters the solid dissolution with the C₂F, CF and CF₂ phases, as indicated in the shaded region of Figure 16. In this research [90] it was observed that silica does not react with Fe₂O₃ or CaO and remains inert until SFCA start to form above 1050 °C.

Research has been carried out [91] on the formation of 2CaO·Fe₂O₃ at 1000 °C from a stoichiometric mixture of Fe₂O₃ and CaCO₃. Fe₂O₃ is reduced to Fe₃O₄ and FeO before the calcination of limestone starts, as a function of the partial pressure of oxygen (P(O₂)), which is determined according to the CO content in the CO+CO₂ reducing mixture. The following order is found for the reaction rate of iron oxide with lime, for the formation of dicalcium ferrite: FeO > Fe₃O₄ > Fe₂O₃.

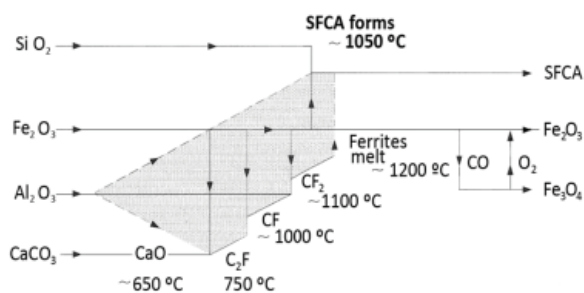
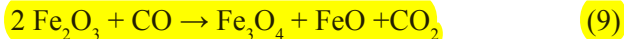


Figure 16. Schematic diagram showing the reaction sequences involved in the formation of SFCA

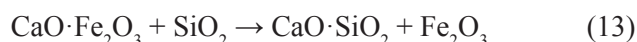
Throughout the process, the iron oxide can simultaneously be reduced by carbon monoxide produced in the partial combustion of coke-coal [92,93]:



Fe₃O₄ can oxidise to Fe₂O₃. FeO can oxidise to Fe₃O₄ or Fe₂O₃, and can initiate with outside energy (carbon or solar), low melting point slag formation reactions [92,94]:



Silica from the iron ore can react with the molten ferrite to form calcium silicates and precipitate hematite or magnetite, depending on the p_{O2} in the reaction system, together with the silicate formed [71,95]:



The sequence of reactions shown above has been widely studied due to its importance in sintering.

In one study [96] calcium ferrite CF samples and CF + Al₂O₃ and CF + SiO₂ samples have been sintered. It was determined that the addition of alumina is more effective to dissolve the hematite in CF, and the addition of silica is more effective to raise the CF formation rate. CF₂ and CF₂ + Al₂O₃ (3-9%) + SiO₂ (1-7%) samples have been sintered to prepare SFCA [97], monitoring the evolution of these processes by XRD. Alumina solubility in CF₂ at 1250 °C is 5-7% and silica solubility is 2-4%. Monoclinic structure CF₂ changes to triclinic when it reacts with Al₂O₃ and SiO₂ to form SFCA. The addition of SiO₂ at 1200 °C causes partial decomposition of CF₂ into calcium silicates [97]. As the Al₂O₃/SiO₂ ratio increases, hematite formation decreases and SFCA formation increases. The Fe³⁺ ion (radius 0.65 Å) in tetrahedral centres is replaced by smaller ions (Si⁴⁺, 0.40 Å and Al³⁺, 0.54 Å), in such a way that the unit cell volume tends to decrease as more Si⁴⁺ and Al³⁺ are added to the CF₂.

Research has been carried out [98] on the penetration of a slag tablet of calcium ferrite (CF) and of CF with addition of 3% and 5% SiO₂ or Al₂O₃ on a hematite substrate, with 5% and 15% porosity. The penetration depth of CF melts into dense hematite (5% porosity)

was depressed by the addition of SiO_2 or Al_2O_3 . The penetration of CF-based melts, did not take place and melts/hematite interface moved down by dissolution of solid hematite into these melts. The penetration into porous hematite (15% porosity) was 10 times deeper than the case of dense hematite.

In research [99] into SFCA stability between 1240 and 1390 °C, 73 specimens have been prepared from mixtures of four ores in the Fe_2O_3 -CaO- Al_2O_3 - SiO_2 (FCAS) system in order to manufacture SFCA. The lower temperature limit of 1240 °C was selected on the basis that it is the lowest anticipated SFCA melting temperature. It is estimated that the SFCA solid solution will completely decompose at around 1480 °C.

The crystalline structure of Mg-rich SFCA (SFCAM) has been researched [100]. SFCAM have been synthesised from chemical reagents, with different MgO contents, and it is established that, similarly to SFCA, the structure of the SFCAM phase is iso-structural with aenigmatite $\text{X}_2\text{Y}_6\text{Z}_6\text{O}_{20}$. The octahedral sites are occupied by Ca, Fe, Mg and Al; the tetrahedral sites by Fe, Al and Si. The composition $\text{Ca}_2(\text{Ca,Fe,Mg,Al})_6(\text{Fe,Al,Si})_6\text{O}_{20}$ can be established for SFCAM. It has been determined that the chemical formula of SFCA can be written as $5\text{CaO} \cdot 2\text{SiO}_2 \cdot 9(\text{Fe,Al})_2\text{O}_3$ [97,101]. SFCA form by a solid-liquid reaction between hematite and the Fe_2O_3 -CaO melt, with the subsequent assimilation of SiO_2 and Al_2O_3 in this melt. In other research it has been determined that there is good agreement between the chemical composition of calcium ferrites and the aenigmatite formula [102].

REFERENCES

- [1] Dawson, P. R., *Ironmaking Steelmaking*, vol. 20, pp. 137-143, 1993.
- [2] De la Torre, L., *Dyna*, vol. 78, pp. 227-234, 2011.
- [3] Goldring, D. C., Jukes L. M. and Fray, T. A. T., *Proc. 5th Int. Symp. on Agglomeration*, Brighton, United Kingdom, 1989, The Institution of Chemical Engineers (ICHEM), pp. 425-439.
- [4] Cumming, M. A. and Thurlby, J. A., *Ironmaking Steelmaking*, vol. 17, pp. 245-254, 1990.
- [5] Cappel, F., *ISS Ironmaking Conf. Proc.*, vol. 50, pp. 525-539, 1991.
- [6] Cores, A., Babich, A., Muñiz, M., Ferreira, S. and Mochón, J., *ISIJ Int.*, vol. 50, pp. 1089-1098, 2010.
- [7] Restrepo, O. J., Vásquez, C. F. and Bustamente, M. O., *Dyna*, vol. 75, pp. 163-170, 2008.
- [8] Yamaoka, Y., Nagaoka, S., Yamada, Y. and Ando, R., *Trans. Iron Steel Inst. Jpn.*, vol. 14, pp. 185-194, 1974.
- [9] Dawson, P. R., *SEAJSI Q.*, vol. 16, pp. 23-42, 1987.
- [10] Napoleão, A., Pinheiro, P., Caparoli, L., Oliveira, D. L. A., Fujikawa, L. and Vervenee, R., *Proc. 3rd Int. Conf. on Sci. and Tech. of Ironmaking*, VDEh, Düsseldorf, Germany, pp. 127-132, 2003.
- [11] Otomo, T., Taguchi, N. and Kasai, E., *ISIJ Int.*, vol. 36, pp. 1338-1343, 1996.
- [12] Yang, L. X., Witchard, D. and Yu, Z. N., *ISIJ Int.*, vol. 40, pp. 647-653, 2000.
- [13] Bergstrand, R. C., Waters, A. G. and Clout, J. M. F., *Proc. 3rd Int. Conf. on Sci. and Tech. of Ironmaking*, VDEh, Düsseldorf, Germany, pp. 424-429, 2003.
- [14] Storkey, A., Doecke, A. and Whaanga, A., *Applied Earth Science. Trans. Inst. Min. Metall. B*, vol. 119, pp. 2-11, 2010.
- [15] Kawaguchi, T. and Usui, T., *ISIJ Int.*, vol. 45, pp. 414-426, 2005.
- [16] Kasai, E., Komarov, S., Nushiro, K. and Nakano, M., *ISIJ Int.*, vol. 45, pp. 538-543, 2005.
- [17] Otomo, T., Takasaki, Y. and Sato, H., *ISIJ Int.*, vol. 49, pp. 659-666, 2009.
- [18] Loo, C. E., *ISIJ Int.*, vol. 45, pp. 436-448, 2005.
- [19] Okazaki, J. and Higuchi, K., *ISIJ Int.*, vol. 45, pp. 427-435, 2005.
- [20] Bergstrand, R. C., Khosa, J., Waters, A. G. and Garden, J., *ISIJ Int.*, vol. 45, pp. 492-499, 2005.
- [21] Otomo, T., Tasaki, Y. and Kawaguchi, T., *ISIJ Int.*, vol. 45, pp. 532-537, 2005.
- [22] Hsieh, L. H., *Proc. on Iron and Steel Tech. Conf. Indianapolis, IN, USA. Association for Iron and Steel Tech.*, Warrendale, PA, USA, vol. 1, pp. 207-214, 2007.

- [23] Hsieh, L. H., *ISIJ Int.*, vol. 45, pp. 551-559, 2005.
- [24] Ramanaidou, E. R. and Morris, R. C., *Applied Earth Science. Trans. Inst. Min. Metall. B*, vol. 119, pp. 56-59, 2010.
- [25] Shigema, A., *Yawata Tech. Rep.* No. 264, September, pp. 111-117, 1968.
- [26] Kodama, T., Artani, F. and Tanaka, T., *Trans. Iron Steel Inst. Jpn.*, vol. 22, B296, 1982.
- [27] Loo, C. E., *Ironmaking Steelmaking*, vol. 18, pp. 33-40, 1991.
- [28] Peters, K. H., Beer, H., Kropla, H. W. and Rinne, K., *Proc. 5th Int. Symp. on Agglomeration*, Brighton United Kingdom, The Institution of Chemical Engineers (ICHEM), pp. 51-70, 1989.
- [29] Lovel, R. R., Vining, K. R. and Dell'amico, M., *ISIJ Int.*, vol. 49, pp. 195-202, 2009.
- [30] Furui, T., Sugawara, K., Kagawa, M., Uno, S., Kamazu, S. M., Fujiwara, T. and Sawamura, A., *Nippon Steel Tech. Rep. (Overseas)*, vol. 10, pp. 36-46, 1977.
- [31] Hida, Y., Sasaki, M., Sato, K., Kagawa, M., Miyazaki, T., Soma, H., Naito, H. and Taniguchi, M., *Nippon Steel Tech. Rep. (Overseas)*, vol. 35, pp. 59-67, 1987.
- [32] Litster, J. D. and Waters, A. G., *Powder Technol.*, vol. 55, pp. 141-151, 1988.
- [33] Litster, J. D., Waters, A. G. and Nicol, S. K., *Trans. Iron Steel Inst. Jpn.*, vol. 26, pp. 1036-1044, 1986.
- [34] Kawachi, S. and Kasama, S., *ISIJ Int.*, vol. 49, pp. 637-644, 2009.
- [35] Rankin, W. J., *Proc. 2nd Int. Symp. on "Benefaction and Agglomeration"*, 1986, Bhubaneswar, India, Institute of Metals, pp. 107-117.
- [36] Wild, R. and Dixon, K. G., *Proc. 1st Int. Symp. on Agglomeration*, 1962, New York, USA, Wiley-Interscience, pp. 565-580.
- [37] Iwamoto, M., Hasimoto, K., Inaba, M., Kobayashi, T., Komatsu, O. and Shimizu, M., *Nippon Kokan Tech. Rep. (Overseas)*, vol. 50, pp. 1-8, 1987.
- [38] Stubel, J. F. and Durko, D. P., *ISS Ironmaking Conf. Proc.*, vol. 47, pp. 657-659, 1988.
- [39] Kurosawa, S., Fukuyo, H., Komatsu, O., Sakamoto, N. and Yamoka, J., *ISS Ironmaking Conf. Proc.*, vol. 48, pp. 451-458, 1989.
- [40] Kawaguchi, T., Kuriyama, K., Satoh, S., Takata, K. and Miyake, T., *Proc. 6th Int. Iron and Steel*, Nagoya, Japan, ISIJ, pp. 31-39, 1990.
- [41] Hida, Y., Okazaki, J. and Nakamura, K., *Proc. 6th Int. Iron and Steel Cong.*, Nagoya, Japan, ISIJ, pp. 40-47, 1990.
- [42] Haga, T., Oshio, A., Shibata, D., Kasama, S., Kozono, T. and Hida, Y., *Proc. 4th European Cokemaking and Ironmaking Cong.*, Paris, France, vol. 1, ATS, Paris, pp. 118-125, 2000.
- [43] Shatoka, V., Korobeynikov, I., Maire, E. and Adrien, J., *Ironmaking Steelmaking*, vol. 36, pp. 416-420, 2009.
- [44] Khosa, J. and Manuel, J., *ISIJ Int.*, vol. 47, pp. 965-972, 2007.
- [45] Shatoka, V., Korobeynikov, I., Maire, E., Grémillard, L. and Adrien, J., *Ironmaking Steelmaking*, vol. 37, pp. 313-318, 2010.
- [46] Mou, J. L., Sun, Y. M., Chen, Y. Ch., Liao, Ch. W. and Tarng, Y. S., *ISIJ Int.*, vol. 47, pp. 1280-1283, 2007.
- [47] Nakano, M., Kawaguchi, T., Kasama, S., Inazumi, T., Torii, J. and Nakano, T., *ISIJ Int.*, vol. 37, pp. 339-344, 1997.
- [48] Lv, X. W., Bai, C. G., Qiu, G., Zhang, S. and Hu, M., *ISIJ Int.*, vol. 50, pp. 695-701, 2010.
- [49] Lv, X. W., Bai, C. G., Zhou, C. Q., Xie, H. and Shi, R. M., *Ironmaking Steelmaking*, vol. 37, pp. 407-413, 2010.
- [50] Maeda, T., Fukumoto, Ch., Matsumura, T., Nishioka, K. and Shimizu, M., *ISIJ Int.*, vol. 45, pp. 477-484, 2005.
- [51] Lwamba, E. and Garbers-Craig, A. M., *J. S. Afr. Inst. Min. Met.*, vol. 108, pp. 293-300, 2008.
- [52] Oboso, A., Shouho, T., Tajiri, K., One, K. and Matsumura, M., *Proc. 2nd Int. Cong. on Sci. and Tech. Ironmaking. ISS Ironmaking Conf. Proc.*, vol. 57, pp. 1327-1336, 1998.
- [53] Nandy, B. and Gupta, S. S., *ISS Ironmaking Conf. Proc.*, vol. 59, pp. 241-247, 2000.
- [54] Umadevi, T., Deodhar, A. V., Mahapatra, P. C., Prabhu, M. and Ranjan, M., *Steel Res. Int.*, vol. 81, pp. 716-723, 2010.

- [55] Oyama, N., Sato, H., Takeda, K., Ariyama, T., Masumoto, S., Jinno, T. and Fuji, N., *ISIJ Int.*, vol. 45, pp. 817-826, 2005.
- [56] Shibata, D., Haga, T., Oshio, A., Kasama, S., Yamamura, Y. and Watanabe, K., *CAMP-ISIJ*, vol. 10, pp. 804-811, 1997.
- [57] Umadevi, T., Deodar, A. V., Mahapatra, P. C., Prabhu, M. and Ranjan, M., *Steel Res. Int.*, vol. 80, pp. 686-692, 2009.
- [58] Nakano, M., Katayama, K. and Kagama, S., *ISIJ Int.*, vol. 50, pp. 1054-1058, 2010.
- [59] Toda, H., Senzaki, T., Isozaki, S. and Kato, K., *Trans. Iron Steel Inst. Jpn.*, vol. 24, pp. 187-196, 1984.
- [60] Ishikawa, Y., Kase, M., Sasaki, M., Satoh, K. and Sasaki, S., *ISS Ironmaking Conf. Proc.*, vol. 41, pp. 80-89, 1982.
- [61] Kurihara, J., Fukuda, A., Tanaka, S. and Nigo, S., *ISS Ironmaking Conf. Proc.*, vol. 42, pp. 71-78, 1983.
- [62] Dawson, P. R., *Proc. 4th Int. Symp. on Agglomeration*, Toronto, On, Canada. Ed. C. E. Capes, Iron and Steel Soc. of AIME, Warrendale, PA, USA, pp. 243-250, 1985.
- [63] Dawson, P. R., Ostwald, J. and Hayes, K. M., *Proc. Australasia Inst. Min. Metall.*, vol. 289, pp. 163-169, 1984.
- [64] Patisson, F., Bellot, J. P., Ablitzer, D., Marlière, E., Dulcy, C. and Steiler, J. M., *Ironmaking Steelmaking*, vol. 18, pp. 89-95, 1991.
- [65] Yasumoto, S. and Tanaka, S., *Kawasaki Steel Tech. Rep.*, vol. 5, pp. 1-8, 1982.
- [66] Nakajima, R., Kurosawa, S., Fukuyo, H. and Yamaoka, Y., *Proc. 6th Int. Iron and Steel Cong.*, Nagoya, Japan, ISIJ, pp. 163-170, 1990.
- [67] Marlière, E., Dulcy, C., Huguet, C. and Leblanc, O., *Proc. 3rd European Cokemaking and Ironmaking Cong.*, Gent, Belgium, Vol. 1. Ed. CRM, Liège, Belgium, pp. 202-208, 1996.
- [68] Yang, W., Ryu, C., Choi, S., Lee, D. and Huh, W., *ISIJ Int.*, vol. 44, pp. 492-499, 2004.
- [69] Mitterlehner, J., Loeffler, G., Winter, F., Hofbauer, H., Schid, H., Zwittag, E., Buergler, T. H., Pammer, O. and Stiasny, H., *ISIJ Int.*, vol. 44, pp. 11-20, 2004.
- [70] Ishikawa, Y., Shimomura, Y., Sasaki, M., Hida, Y. and Toda, H., *ISS Ironmaking Conf. Proc.*, vol. 42, pp. 17-29, 1983.
- [71] Matsuno, F. and Harada, T., *Trans. Iron Steel Inst. Jpn.*, vol. 21, pp. 318-325, 1981.
- [72] Hsieh, L. H. and Whiteman, J. A., *ISIJ Int.*, vol. 29, pp. 625-634, 1989.
- [73] Hsieh, L. H. and Whiteman, J. A., *ISIJ Int.*, vol. 29, pp. 24-32, 1989.
- [74] Formoso, A., Moro, A., Fernández-Pello, G., Menéndez, J. L., Muñiz, M. and Cores, A., *Ironmaking Steelmaking*, vol. 30, pp. 447-460, 2003.
- [75] Cores, A., Mochón, J., Ruiz-Bustinza, I. and Parra, R., *Rev. Metal. Madrid*, vol. 46, pp. 249-259, 2010.
- [76] Propster, M. A. and Szekely, J., *Ironmaking Steelmaking*, vol. 6, pp. 209-220, 1979.
- [77] Wakamaya, S., Kanamaya, Y. and Okuno, Y., *Ironmaking Steelmaking*, vol. 6, pp. 261-267, 1979.
- [78] Busby N. J., Fray, T. A. T. and Goldring, D. C., *Ironmaking Steelmaking*, vol. 21, pp. 229-236, 1994.
- [79] Cores A., Saiz de Ayala, J., Mochón, J., Ruiz-Bustinza, I. and Parra, R., *Rev. Metal. Madrid*, vol. 46, pp. 293-307, 2010.
- [80] Bakker, T. and Heerema, R. H., *ISS Ironmaking Conf. Proc.*, vol. 56, pp. 365-373, 1997.
- [81] Bakker, T. and Heerema, R. H., *Proc. 2nd Int. Cong. on Sci. and Tech. Ironmaking*. ISS Ironmaking Conf. Proc., vol. 57, pp. 1597-1608, 1998.
- [82] Singh, B. N., De, A., Rawat, Y. F., Das, R. C. and Chatterjee, A., *Iron Steel Inter.*, August, pp. 135-141, 1984.
- [83] Nandy, B., Chandra, S., Bhattacharjee, D. and Ghosh, D., *Ironmaking Steelmaking*, vol. 33, pp. 111-119, 2006.
- [84] Barnaba, P., *Ironmaking Steelmaking*, vol. 12, pp. 53-63, 1985.
- [85] Hsieh, L. H. and Liu, K. Ch., *Proc. 2nd Int. Cong. on Sci. and Tech. Ironmaking*. ISS Ironmaking Conf. Proc., vol. 57, pp. 1623-1632, 1998.
- [86] Pal, S., Chandra, N., Mishra, U. N., Singh, R. N. and Mediratta, S. R., *Proc. 2nd Int. Cong. on Sci. and Tech.*

Ironmaking. ISS Ironmaking Conf. Proc., vol. 57, pp. 1615-1621, 1998.

[87] Matsumura, M., Hoshi, M. and Kawaguchi, T., *ISIJ Int.*, vol. 45, pp. 594-602, 2005.

[88] Ueno, H., Yamaguchi, K., Orimoto, T., Okuno, Y., Matsunaga, S., Oda, H., Amano, S. and Nose, M., *1st Int. Cong. on "Science and technology of ironmaking"*, Sendai, Japan, ISIJ, pp. 217-222, 1994.

[89] Loo, C. E., Matthews, L. T. and O'Dea, D. P., *ISIJ Int.*, vol. 51, pp. 930-938, 2011.

[90] Scarlett, N. V. Y., Pownceby, M. I., Madsen, I. C. and Christensen, A. N., *Metall. Mater. Trans. B*, 35B, pp. 929-936, 2004.

[91] Jeon, J. W., Jung, S. M. and Sasaki, Y., *ISIJ Int.*, vol. 50, pp. 1064-1070, 2010.

[92] Egundebi, G. O. and Whiteman, J. A., *Ironmaking Steelmaking*, vol. 16, pp. 379-385, 1989.

[93] Rojas, A. F. and Barraza, J. M., *Dyna*, vol. 75, pp. 113-122, 2008.

[94] Ruiz-Bustanza, I., Cañadas, I., Rodríguez, J., Mochón, J., Verdeja, L. F., García-Carcedo, F. and Vázquez, A. J., *Steel Research Int.* vol. 84, pp. 207-217, 2013.

[95] Matsuno, F., *Trans. Iron Steel Inst. Jpn.*, vol. 19, pp. 595-604, 1979.

[96] Maeda, T., Nishioka, K., Nakashima, K. and Shimizu, M., *ISIJ Int.*, vol. 44, pp. 2046-2051, 2004.

[97] Kim, H. S., Park, J. H. and Cho, Y. C., *Ironmaking Steelmaking*, vol. 29, pp. 266-270, 2002.

[98] Yoshimura, S., Kurosawa, K., Gonda, Y., Sukenaga, S., Saito, N. and Nakashima, K., *ISIJ Int.*, vol. 49, pp. 687-692, 2009.

[99] Patrick, T. R. C. and Pownceby, M. I., *Metall. Mater. Trans. B*, 33B, pp. 79-89, 2002.

[100] Sugiyama, K., Monkawa, A. and Sugiyama, T., *ISIJ Int.*, vol. 45, pp. 560-568, 2005.

[101] *Joint Committee on Powder Diffraction Standards (JCPDS)*, Swarthmore, PA, USA, International Centre for Diffraction Data, (JCPDS file 33-0250), 1983.

[102] da Costa, E. and Coheur, J. P., *Ironmaking Steelmaking*, vol. 22, pp. 223-226, 1995.